# Piezoelectric MEMS for Frequency Control and Sensing

Yao Zhu, Bhattacharya Shashwat, Wenjia Yang, Li Chen, Ying Zhang, Chen Liu
Institute of Microelectronics, Agency for Science, Technology and Research (A*STAR), Singapore
zhuya@ime.a-star.edu.sg

***This paper reviews key piezoelectric MEMS works for the applications of RF signal processing and sensing. The material, device design, and performance of AlN and Sc-doped AlN piezoelectric MEMS devices are discussed. Different process platforms and their applications in frequency control and sensing applications are also presented. Finally, the trends in piezoelectric MEMS research are summarized and future work is recommended.***

***Keywords—piezoelectric, MEMS, frequency, sensing, resonators, filters, monolithic.***

## I. Background

The piezoelectric MEMS transducer plays a vital role in the translation of acoustic vibrations to electrical signals. It can serve as an enabling technology for a variety of domains, including radio frequency (RF) communication systems [1], inertial sensors [2], energy harvesting [3], bio-applications [4], and acoustic wavefront computing [5]. The smart eco-space of the Industrial Revolution 4.0 will consist of many piezoelectric transducers. The semiconductor process enables MEMS to realize different products, such as sensors, actuators, and signal processing units, at low cost, small form factor, and with controlled dimensions and performance.

In comparison to the large industry usage of capacitive transduction, piezoelectric transduction has the advantages of the lower driving voltage, small size, immunity to parasitic capacitance, and absence of fine gaps. However, it does encounter a challenge in the enhancement of the coupling coefficient. This is because the material property is highly dependent on its thickness, stack configuration, and fabrication process. The improvement of this transduction efficiency is driven by the choice of material properties, a robust fabrication platform, and device design innovations. This work summarizes these three aspects with a focus on AlN/Scandium-doped AlN piezoelectric transducers.

## II. Review

### A. Material Choice

Scandium-doped AlN is the most promising material and possesses many outstanding features. Doping with scandium improves the piezoelectric constant of AlN by four to five times [6] compared to undoped AlN. The higher value of the coupling coefficient results in an increase in sensor sensitivity and wider filter bandwidth. This improvement also lowers the loss at GHz frequencies leading to a higher signal-to-noise ratio for sensors and sharper roll-off with lower insertion loss for the filter.

The film deposition temperature of scandium-doped AlN is below 400 degrees Celsius, thereby enabling monolithic integration with CMOS [7], ensuring high-yield and cost-effective mass production. In addition to its piezoelectric properties, scandium-doped AlN exhibits notable ferroelectric [8], pyroelectric [9], and electro-optical properties [10]. These properties find applications in tunable RF components [11], ferroelectric memory [12], infrared sensors [13], and photonics devices for data communication [14].

The roadmap for scandium-doped AlN thin film development is towards higher scandium concentration and thinner film thickness. The higher scandium concentration gives a higher coupling coefficient at the cost of defects appearing in the film. These defects appear especially in the form of misoriented grains [15], which can degrade the piezoelectric properties of the film. Thinner thickness degrades the overall crystallinity of the film, which can also degrade the piezoelectric properties. However, the resonator and filter at higher frequencies need these thinner film thicknesses. The current capability of the organization is up to 30% Sc-doped AlN on a 200 mm wafer with near zero defects [16]. The minimum thickness of 20 nm was reported with reasonably good quality. The residual stress control during the $Sc_xAl_{1-x}N$ and metal electrodes needs special consideration. The increase in Sc concentration makes the etching more difficult. To address the issue of selectivity of the piezo layer etch to the bottom electrode, both tapered and vertical etch profile recipe development is necessary as per the application. The usage of thickness trimming provides thickness uniformity control of around 0.1% across the wafer for filter applications. [16]

### B. Robust Fabrication Platform

The choice of the fabrication platform depends on the target application, stack requirement, and method of cavity formation. The three available fabrication platforms for Scandium-doped AlN front-side cavity thin film are $Sc_xAl_{1-x}N$ platform [17], back-side cavity [18], and $Sc_xAl_{1-x}N$ over silicon on nothing platform [19]. Fig. 1 shows the stack configuration of different platforms. The first process is ideal for GHz resonators and filter applications. The cavity is created using front-side vapor HF release [17]. The back-side cavity platform consists of a top electrode, the piezoelectric layer, the bottom electrode layer, a thin (few µm) silicon, and an oxide layer. This platform is ideal for sensors and actuator applications consisting of a silicon

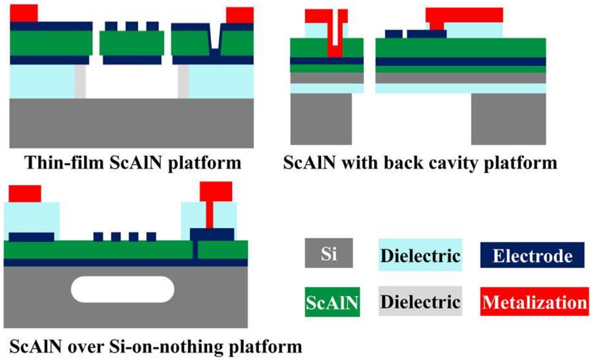


Figure.1 ScAlN MEMS platforms at IME.

device layer. The piezoelectric over silicon on nothing (PSON) platform consists of a similar stack as the previous platform apart from the pre-formed cavity. The pre-formation of the cavity before the bottom electrode deposition uses the silicon migration process [20]. It supports different sizes of cavities, variable thicknesses of silicon device layer within the wafer, and the option to keep the cavity sealed or unsealed.

### *C. Device design innovations*

Resonator and filter design for RF communications require targeting higher frequencies and higher coupling coefficients. For commercially available FBAR, the operational frequency depends on the thickness of the piezoelectric film [21]. To support multiple frequencies on the same wafer without an additional loading layer exploration of different design approaches is necessary. For consistent comparison, different design approaches for AlN material are compared to FBAR with a coupling coefficient of 7.2% at 2.4 GHz as shown in Fig.2. The usage of a lamb wave resonator [22] provides tunability but the coupling coefficient of less than 2% at 2.1 GHz is too low for usage in filter applications. The design innovations to increase the coupling coefficient includes frequency tunability by controlling the electrode design. The use of checkered pattern electrodes [23], laterally coupled alternating thickness mode resonators (LCAT) [17], and coupled bulk acoustic resonators

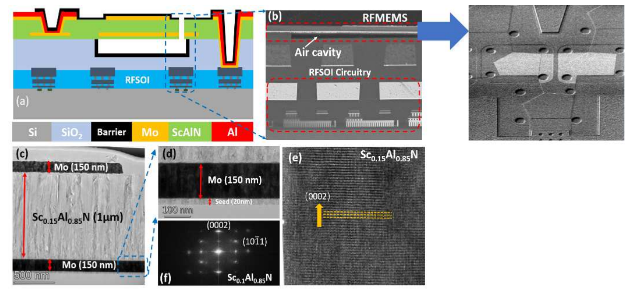


Figure.3 Monolithic integration of Thin-film ScAlN MEMS platforms on RFSOI [7](©2022 IEEE).

(CBAR) [24] provided tunability along with performance enhancement. For checkered pattern electrodes shown in Fig.3(b), the device provides a coupling coefficient of 5% at a lower frequency of 285 MHz [25]. Further, the removal of redundant areas of AlN can boost the coupling coefficient to 8.7% at 2.3 GHz. The LCAT operates at a frequency of 2.3 GHz with a coupling coefficient of 6.3%, which is close to FBAR frequency. The major drawback of this design lies in the need for the pattern of the bottom electrode which makes the deposition of AlN film over it challenging. CBAR solves this problem and can achieve a coupling coefficient of 8.3% at 2.5 GHz which is higher than the FBAR.

### *D. Monolithic integration on RFSOI*

As the $Sc_xAl_{1-x}N$ deposition has a thermal budget compatible with the CMOS process, monolithic integration on the RFSOI circuit is possible [7]. This integration enables vertical integration in comparison to the two-chip integration. It provides a smaller device footprint and a reduction in interconnection and packaging loss. The monolithic integration consists of a series connection of a 2.5 GHz BAW filter with a single pole double throw (SPDT) switch. The integrated device has a filter response close to the standalone filter response. The filter response provides high bandwidth of 130 MHz and insertion loss close to 3.5 dB. The temperature coefficient of frequency (TCF) of -20 ppm is comparable to the standalone filter. The power handling capacity of the integrated device is 30 dBm.

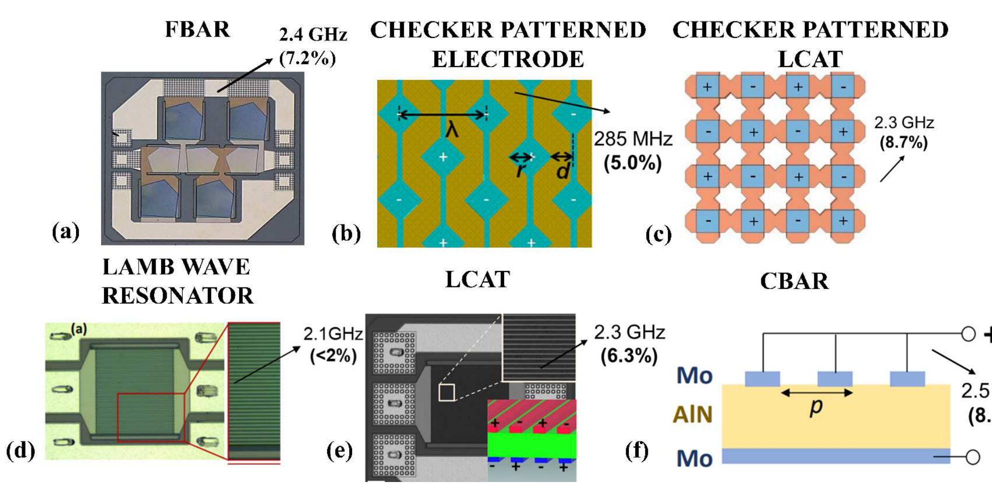


Figure.2 Different design innovations on the thin-film ScAlN MEMS platforms (a) FBAR, (b) Checker Patterned Electrode [25] (©2015 APL), (c) Checkered Patterned LCAT [23] (©2018 IEEE), (d) Lamb Wave Resonator [22](©2018 IEEE), (e) LCAT [17](©2016 IEEE), and (f) CBAR [24](©2019 IEEE).

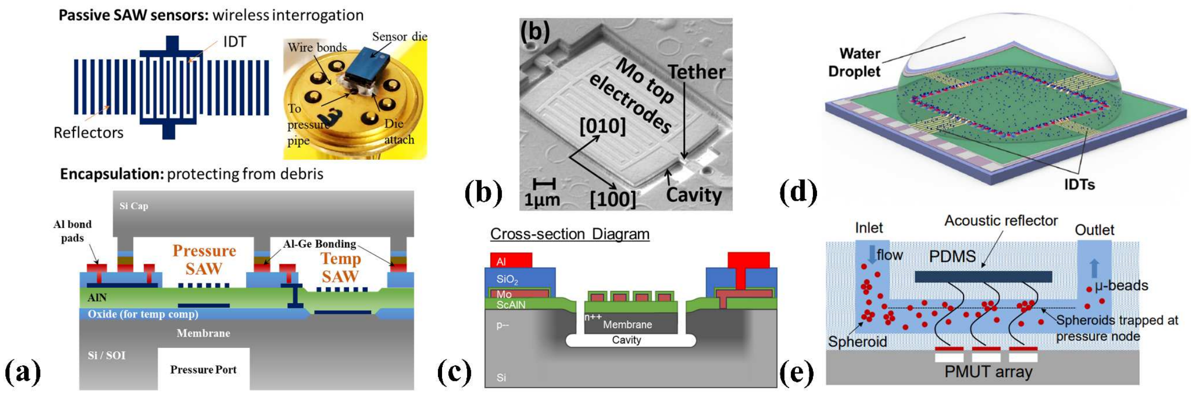


Figure.4 Sensor Applications using ScAlN MEMS platforms (a) Passive SAW Sensor using ScAlN back cavity platform [18](©2021 IEEE), (b) Temperature compensated resonator using PSON process [26](©2021 IEEE), (c) PSON process cross-section with air-exposed cavity [26](©2021 IEEE), (d) IDT based Microfluidic device using PSON [29](©2023 RSC), (e) PMUT based microfluidic device using PSON [30](©2022 IEEE).

### E. *Sensor applications*

This section presents some sensor applications using various process platforms. The back-cavity platform demonstrates a SAW-like passive sensor [18] that uses one device to integrate pressure sensing, temperature sensing, and wireless interrogation function. The antenna receives an interrogating signal at a port. The frequency shift estimation of this return signal enables the pressure and temperature measurement. The pressure sensor has a back-side cavity, and the temperature sensor is unreleased. As the temperature and pressure sensors follow different coefficients, the two sensors can decouple the temperature and pressure data.

The PSON process can provide a fully sealed or air-exposed cavity as per the application. This platform also provides the option to dope the silicon membrane and use it as the bottom electrode. The MHz to GHz resonators can use this single-crystal doping and device orientation change to achieve a tremendous reduction in the TCF [26].

The piezoelectric micromachined ultrasonic transducer (PMUT) can use the PSON platform for the application of high-resolution ranging [27] and remote temperature sensing [28]. It uses the principle of time-of-flight for the applications. For high-resolution ranging, the PMUT devices placed on top of a shaker system are a few centimeters apart. The shaker actuates at 50 or 100 Hz along with introducing the movement of the shaker plate close or away from the PMUT device. It can resolve around 4.3 µm resolution with a measurement time of 0.5 ms. For remote sensing, the device measures the temperature dependency of the ultrasound signal velocity that propagates through a medium. It measures the temperature of the medium and not the temperature of the object. The system consists of a transmitter and a receiver PMUT with a variable separation of around 1 cm. The peak of the autocorrelated peak and cross-correlated peak are different when the temperature changes. An algorithm extracts the temperature change corresponding to this difference.

The PSON process can create chip-scale microfluidic devices. This process can make a fully sealed cavity which is very suitable for operation in a liquid environment. The two demonstrations of microfluidic devices using this platform are inter-digitated transducer (IDT) [29] and PMUT based [30]. The IDT-based device uses the IDT to provide excitation across the channel formed using the predefined cavity. The IDT can make the particle spin and steering of the particle. For the second device design, the particle excitation uses PMUT. In comparison to the IDT in which the actuation is limited to a certain location, the use of PMUT can embed the entire channel beneath the PMUT actuator. The device can achieve a very precise 2-dimensional localized pressure control in a compact size.

## III. Conclusions

This paper gives an overview of the different AlN platforms in the organization. It shares the different strategies to meet the specification pertaining to the application. It discusses the gaps between existing technology/works versus desired performance for different applications regarding the robust process platform, design innovations, and material choice. In the future, efforts to reduce film thickness while maintaining film quality and application-specific design innovation can be pursued. The research will focus to reduce the turnaround time from design conceptualization to MEMS prototyping, low-volume fabrication, and high-volume fabrication. Further work in the monolithic integration for 5G and Wi-Fi commands a big potential market for MEMS products. Exploration of the ferroelectric properties of the Sc-doped AlN can open the door to enhancement in the big memory market. The timing market has always had a big share of the MEMS. Other applications such as acousto-optic modulators, quantum computing, laser imaging detection, and ranging (LIDAR), etc. need more exploration

## Acknowledgment

The funding support for these works is given by the Science and Engineering Research Council of A*STAR (Agency for Science, Technology, and Research) Singapore, under Grant No. A20G9b0135 and A18A4b0055

## REFERENCES

[1] H. A. C. Tilmans, W. DeRaedt, and E. Beyne, “MEMS for wireless communications: 'from RF-MEMS components to RF-MEMS-SiP'”, *Journal of Micromechanics and Microengineering*, vol. 13, no. 4, pp. S139–S163, Jun. 2003.

[2] S.Tadigadapa and K. Mateti, “Piezoelectric MEMS sensors: state-of-the-art and perspectives”, *Measurement Science and Technology*, vol. 20, no. 9, pp. 092001, Jul. 2009.

[3] J. Wang, Z. Chen, Z. Li, J. Jiang, J. Liang and X. Zeng, "Piezoelectric Energy Harvesters: An Overview on Design Strategies and Topologies," *IEEE Transactions on Circuits and Systems II: Express Briefs*, vol. 69, no. 7, pp. 3057-3063, July 2022.

[4] W. Pang, H. Zhao, E. S. Kim, H. Zhang, H. Yu, and X. Hu, "Piezoelectric microelectromechanical resonant sensors for chemical and biological detection," *Lab on a Chip*, vol. 12, no. 1, pp. 29-44, Nov. 2011.

[5] Z. Yang, X. H. M. Tan, V. P. Bui, D. S. -H. Chen, K. T. -C. Chai, C. E. Png, and A. Lal, "Effect of Tapered Angle on BAW Transducer Performance for Ultrasonic Wavefront Computing," *Proceedings*, 2022 IEEE International Ultrasonics Symposium (IUS), Venice, Italy, 2022, pp. 1-3.

[6] M. Akiyama, K. Kano, and A. Teshigahara, "Influence of growth temperature and scandium concentration on piezoelectric response of scandium aluminum nitride alloy thin films," *Applied Physics Letters*, vol. 95, no. 16, pp. 162107, Oct. 2009.

[7] Y. Zhang, X. Wang, C. Liu, E. Y. Z. Woo, W. Yang, Q. Zhang, H. Lin, D. Yan, R. M. Kumarasamy, B. Chen, N. Wang, and Y. Zhu, "3D Monolithic Integration of ScAlN-based GHz MEMS Acoustic Filters on 200mm RFSOI Wafer," *Proceedings*, 2022 International Electron Devices Meeting (IEDM), San Francisco, CA, USA, 2022, pp. 16.2.1-16.2.4.

[8] C. Li, L. Chen, M. Li, W. Song, W. Wang, Z. Wang, N. Wang, and Z. Yao, "Scandium-Doped Aluminum Nitride for Acoustic Wave Resonators, Filters, and Ferroelectric Memory Applications," *ACS Applied Electronic Materials*, vol. 5, no. 2, pp. 612-622, Feb. 2023.

[9] G.E. Stan, M. Botea, G.A. Boni, I. Pintilie, and L. Pintilie, "Electric and pyroelectric properties of AlN thin films deposited by reactive magnetron sputtering on Si substrate," *Applied Surface Science*, vol. 353, no. 1, pp. 1195-1202, Oct. 2015.

[10] N. Li, C. Ho, S. Zhu, Y. Fu, Y. Zhu, and L. Lee, "Aluminium nitride integrated photonics: a review," *Nanophotonics*, vol. 10, no. 9, pp. 2347-2387, Jun. 2021.

[11] M. Park and A. Ansari, "Tunable TE-Mode Resonators based on Ferroelectric AlScN Thin Films for RF Applications," *Proceedings*, 2022 Joint Conference of the European Frequency and Time Forum and IEEE International Frequency Control Symposium (EFTF/IFCS), Paris, France, 2022, pp. 1-2.

[12] R. H. Olsson, Z. Tang, and M. D'Agati, "Doping of Aluminum Nitride and the Impact on Thin Film Piezoelectric and Ferroelectric Device Performance," *Proceedings*, 2020 IEEE Custom Integrated Circuits Conference (CICC), Boston, MA, USA, 2020, pp. 1-6.

[13] M. Moosavifar, A. Ansari, and M. Rais-Zadeh, "An AlN-on-Si resonant IR sensor array with a large temperature coefficient of frequency," *Proceedings*, 2016 IEEE SENSORS, Orlando, FL, USA, 2016, pp. 1-3.

[14] B. Dong, Q. Shi, T. He, S. Zhu, Z. Zhang, Z. Sun, Y. Ma, D.-L. Kwong, and C. Lee, "Wearable Triboelectric/Aluminum Nitride Nano-Energy-Nano-System with Self-Sustainable Photonic Modulation and Continuous Force Sensing," *Advanced Science*, vol. 7, no. 15, pp. 1903636, Aug. 2020.

[15] C. Liu, M. Li, B. Chen, Z. Ying, Y. Zhu, and N. Wang, " Evaluation of the impact of abnormal grains on the performance of Sc0.15Al0.85N-based BAW resonators and filters," *Journal of Micromechanics and Microengineering*, vol. 32, no. 3, pp. 034002, Jan. 2022.

[16] C. Liu, M. Li, N. Wang, and Y. Zhu, "Sub-100nm Al0.7Sc0.3N Thin Films for Next Generation Bulk Acoustic Wave Resonators and Filters," *Proceedings*, 2022 IEEE International Ultrasonics Symposium (IUS), Venice, Italy, 2022, pp. 1-3.

[17] Y. Zhu, N. Wang, C. Sun, S. Merugu, N. Singh, and Y. Gu, “A high coupling coefficient 2.3-GHz AlN resonator for high band LTE filtering application,” *IEEE Electron Device Letters*, vol. 37, no. 10, pp. 1344–1346, Oct. 2016.

[18] E. J. Ng, J. Sharma, E. W. L. Ching, G. Wu, D. Pohl, and O. Vancauwenberghe, "Wafer-Scale Encapsulated Saw Temperature and Pressure Sensors for Harsh Environments," *Proceedings*, 2021 IEEE 34th International Conference on Micro Electro Mechanical Systems (MEMS), Gainesville, FL, USA, 2021, pp. 370-373.

[19] J. Sharma, D.J. Goh, S. Merugu, Y. Koh, S. Ghosh, M. H. Khairy, and E. J. Ng, "Piezoelectric over Silicon-on-Nothing (pSON) process," *Proceedings*, 2021 IEEE International Ultrasonics Symposium (IUS), Xi'an, China, 2021, pp. 1-4.

[20] I. Mizushima, T. Sato, S. Taniguchi, and Y. Tsunashima, "Empty-space-in-silicon technique for fabricating a silicon-on-nothing structure," *Applied Physics Letters*, vol. 77, no. 1, pp. 3290-3292, Nov. 2000.

[21] R. Ruby, “A snapshot in time: The future in filters for cell phones,” *IEEE Microwave Magazine*, vol. 16, no. 7, pp. 46–59, Aug. 2015.

[22] Y. Zhu, N. Wang, G. L. Chua, B. Chen, S. Merugu, N. Singh, and Y. Gu, "Apodization Technique for Effective Spurious Mode Suppression of Aluminum Nitride Lamb Wave Resonators," *Proceedings*, 2018 IEEE International Ultrasonics Symposium (IUS), Kobe, Japan, 2018, pp. 1-4.

[23] Y. Zhu, N. Wang, G. L. Chua, B. Chen, S. Merugu, N. Singh, and Y. Gu, "Quality Factor Improvement of a 2.4GHz AlN Checker Patterned Lamb Wave Resonator by Novel Distributed Anchor Design," *Proceedings*, 2018 IEEE International Ultrasonics Symposium (IUS), Kobe, Japan, 2018, pp. 1-4.

[24] Y. Zhu, N. Wang, B. Chen, and Y. Zhang, "AlN BAW-like Resonators with Patterned Top Electrodes Achieving Coupling Coefficient up to 8% at >2.5GHz," *Proceedings*, 2019 IEEE International Ultrasonics Symposium (IUS), Glasgow, UK, 2019, pp. 93-95.

[25] C. Sun, B. W. Soon, Y. Zhu, N. Wang, S. P. H. Loke, X. Mu, J. Tao, and A. Y. Gu, "Methods for improving electromechanical coupling coefficient in two dimensional electric field excited AlN Lamb wave resonators," *Applied Physics Letters*, vol. 106, no. 25, pp. 253502, Jun. 2015.

[26] S. Ghosh, J. Sharma, E. J. Ng, D. J. Goh, S. Merugu, Y. Koh, and A. Lal, "Reduced TCF, High Frequency, Piezoelectric Contour-Mode Resonators with Silicon-on-Nothing," *Proceedings*, 2021 IEEE International Ultrasonics Symposium (IUS), Xi'an, China, 2021, pp. 1-4.

[27] Y. Koh, D. S. Wai Choong, D. S. -H. Chen, D. J. Goh, S. Ghosh, J. Sharma, S. Merugu, F. Quaglia, M. Ferrera, A. S. Savoia, and E. J. Ng, "High Resolution, High Frequency Ultrasonic Ranging in Air with pMUTs," *Proceedings*, 2021 IEEE International Ultrasonics Symposium (IUS), Xi'an, China, 2021, pp. 1-4.

[28] M. Sarafianou, D. J. Goh, and D. S. Wai Choong, "A Time-of-Flight (ToF) estimation algorithm for ranging using Silicon-On-Nothing pMUTs," *Proceedings*, 2022 IEEE International Ultrasonics Symposium (IUS), Venice, Italy, 2022, pp. 1-4.

[29] P. Vachon, S. Merugu, J. Sharma, A. Lal, E. J. Ng, Y. Koh, J. E.-Y. Lee, and C. Lee, "Microfabricated acoustofluidic membrane acoustic waveguide actuator for highly localized in-droplet dynamic particle manipulation," *Lab on a Chip*, vol. 23, no. 7, pp. 1865-1878, Feb. 2023.

[30] Y. Koh, D. J. Goh, D. S. Wai Choong, W. Chen, D. S. -H. Chen, E. J. Ng, and J. E. -Y. Lee "Trapping of Microbead Spheroids by pMUTs in Microfluidic Channels Embedded with an Acoustic Reflector," *Proceedings*, 2022 IEEE International Ultrasonics Symposium (IUS), Venice, Italy, 2022, pp. 1-4.